An advanced robust fault-tolerant tracking control for a doubly fed induction generator with actuator faults

Samir ABDELMALEK[1,2,*], **Linda BARAZANE**[1], **Abdelkader LARABI**[1]
[1]Laboratory of Electrical & Industrial Systems, Faculty of Electronics and Computers,
University of Science and Technology Houari Boumediene, Bab Ezzouar, Algeria
[2]Solar Equipment Development Unit (UDES), Renewable Energies Development Center (EPST CDER),
Tipaza, Algeria

Abstract: Fault-tolerant controller (FTC) designs for doubly fed induction generators (DFIGs) with actuator faults have recently gained considerable attention due to their important role in maintaining the safety and reliability of DFIG-based wind turbines via configured redundancy. The objective of this paper is to propose a novel active fault-tolerant tracking control strategy for a DFIG subject to actuator faults. The proposed strategy consists of first designing a proportional integral observer (PIO) for simultaneous system states and fault estimation and then secondly the FTC, which depends on the estimated states and faults. The objective of such a controller is to drive the state of the system to track a reference state generated by a reference fault-free model (nominal system). In addition, the main results for stability are demonstrated through a quadratic Lyapunov function, formulated in terms of linear matrix inequalities (LMIs) in order to guarantee the stability of the whole closed-loop system and to reduce the actuator fault effects with noise attenuation. Furthermore, the gain matrices of the FTC and the PIO are computed by solving a set of LMIs using the YALMIP toolbox with the SeDuMi solver. Finally, the simulation results under constant and time-varying actuator faults are provided to show the effectiveness of the developed FTC scheme.

Key words: Doubly fed induction generator, fault-tolerant tracking control, proportional integral observer, actuator faults, linear matrix inequality stability conditions

1. Introduction

The use of the doubly fed induction generators (DFIGs) in large wind turbines (WTs) is growing rapidly [1]. This kind of generator has gained more interest due to its advantages over other generators, such as full variable speed operation, power control capability, robustness, and reduced inverter costs [2–4]. However, this generator can be affected by different kinds of faults, such as open-phase failure, short circuits, current sensor faults, voltage dips, and speed sensor faults [5–7]. These faults can be caused by sensors, actuators, or the system itself [8].

Actuator failures can cause severe performance property deterioration of the generators or even generator instability, leading to serious damage over all of the systems, with important economic losses and safety problems. For these reasons, research on controlling systems with actuator faults is a challenging issue [9]. Therefore, it is an important issue in control system design to study how the controlled system is kept stable, with acceptable

*Correspondence: samir_aut@yahoo.fr

performance levels maintained in the presence of faults affecting the system components [10–13]. It is necessary to design robust control systems that are able to reduce the effect of occurring faults, and to increase the reliability and availability of such systems while providing desirable performances [14]. These latter systems are known as fault-tolerant controller (FTC) systems, as they have the capability to accommodate component faults automatically [15]. Generally, FTC systems are divided into two main groups: active and passive [16,17].

More recently, many studies dealing with the problem of FTC systems have been designed for wind energy conversion systems (WECSs) [18–28]. In [18] an extended state observer-based AFTC scheme was presented, which provides an estimation of system states and fault signals for an offshore WT represented by linear parameter-varying descriptor systems. In [19,20], the authors presented a robust approach for designing a FTC in order to stabilize nonlinear systems affected by sensor faults. In [21,22] a FTC scheme for WECSs was improved efficiently to deal with the problems of disturbance rejection and robust stabilization. In [23,24], the authors presented a FTC scheme for WECs described by T-S fuzzy models with sensor faults using a T-S fuzzy observer to achieve maximization of the power extraction from the generator. Furthermore, in [25,26] the robustness of sliding mode control was used to design a FTC strategy for an offshore WT. In [27] an improved FTC scheme-based current observer for current sensors was presented, which can easily detect and tolerate both hard faults and soft faults of current sensors in DFIGs.

In the literature, few authors have dealt with the trajectory tracking problem for WECSs. For example, the authors in [28] developed a novel scheme for AFTTC for offshore WTs represented by multiple models using T-S fuzzy proportional state estimators augmented with proportional and integral feedback fault estimators. The objective was to estimate different generators and rotor speed sensor faults for compensation purposes. However, the AFTTC for DFIGs with actuator faults and disturbances has not been fully investigated. Hence, the goal of this work consists of the proposition of a novel AFTTC scheme for a DFIG subject to actuator faults and noise measurement. This latter is designed using a proportional integral observer (PIO) combined with a new structure of a fault-tolerant control law. The main contributions of the present study are as follows: 1) the proposed scheme has the capability to provide simultaneous system states and actuator fault estimations by the designed PIO, 2) it allows the driving of the state of the faulty system to track a reference state generated by a reference fault-free model, 3) it has the ability to tolerate and compensate the effect of both constant and time-varying actuator faults based on the estimated faults with the PIO, 4) it guarantees the stability and maintains the nominal performance of the closed-loop system when different actuator faults occur, and 5) the main results of this study are formulated in terms of linear matrix inequalities (LMIs) by using Lyapunov theory.

The rest of this paper is organized as follows: Section 2 presents the modeling of the system under study. Section 3 details the proposed AFTTC scheme. The achieved results are reported in Section 4, where the efficiency of the proposed scheme is investigated in numerical simulation tests. Finally, Section 5 gives a conclusion and perspectives of the main presented in this paper.

2. Modeling of DFIG-based WT

The model of the DFIG-based WT is composed of the three following subsystems: an aerodynamic rotor, drive train, and DFIG, as depicted in Figure 1.

2.1. Aerodynamic rotor model

The mechanical power extracted from the WT can be determined as follows [29,30]:
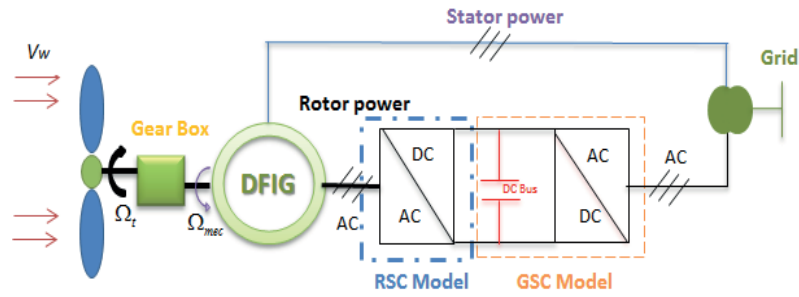
Figure 1. Basic scheme of a DFIG-based WT.

$$P_{wt} = \frac{1}{2}\rho\,\pi\,R^2\,v_w^3 C_p(\lambda, \beta), \tag{1}$$

where ρ represents the air density, R is the rotor blade radius, v_w is the wind speed, and C_p is the power coefficient of the turbine. The following empirical equation is used to compute the value of power coefficient C_p of the turbine [29,31]:

$$C_p(\lambda, \beta) = C_1\left(\frac{C_2}{\lambda_i} - C_3\,\beta - C_4\right)e^{-\frac{C_5}{\lambda_i}} + C_6\lambda, \tag{2}$$

where λ_i relates to λ and β through the following relationship [31]:

$$\frac{1}{\lambda_i} = \frac{1}{\lambda + 0.08\beta} - \frac{0.035}{1 + \beta^3}, \tag{3}$$

where C_1 to C_6 are constant coefficients equal respectively to $C_1 = 0.5176$, $C_2 = 116$, $C_3 = 0.4$, $C_4 = 5$, $C_5 = 21$, and $C_6 = 0.0068$. Figure 2 shows a typical relationship between C_p and λ in the WT model.
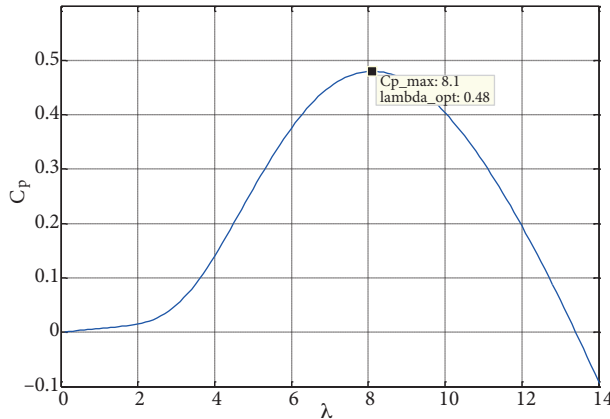

Figure 2. A typical C_p versus λ curve.

2.2. Drive train model

The drive train model is described as follows:

$$\frac{d\omega_r}{dt} = \frac{1}{J_r}(T_e - T_m - \omega_r F), \tag{4}$$

where T_e is the electrical torque of the generator, T_m represents the mechanical torque, ω_r is the angular velocity of the generator, J_r is the aerodynamic rotor inertia, and F is the viscous friction coefficient.

2.3. DFIG dynamics model

The electrical equations of a DFIG are given by [1,3]:

$$\begin{cases} u_{ds} = R_s i_{ds} + \frac{d\phi_{ds}}{dt} - \omega_s \phi_{qs} \\[2mm] u_{qs} = R_s i_{qs} + \frac{d\phi_{qs}}{dt} + \omega_s \phi_{ds} \\[2mm] u_{dr} = R_r i_{dr} + \frac{d\phi_{dr}}{dt} - \omega_r \phi_{qr} \\[2mm] u_{qr} = R_r i_{qr} + \frac{d\phi_{qr}}{dt} + \omega_r \phi_{dr} \end{cases} \tag{5}$$

and

$$\begin{cases} \phi_{ds} = L_s i_{ds} + L_m i_{dr} \\ \phi_{qs} = L_s i_{qs} + L_m i_{qr} \\ \phi_{dr} = L_r i_{dr} + L_m i_{ds} \\ \phi_{qr} = L_r i_{qr} + L_m i_{qs} \end{cases}, \tag{6}$$

where R_s and R_r are the stator and rotor resistances, respectively. L_s and L_r are the stator and inductances, and L_m is the magnetization inductance, i denote currents, φ denotes magnetic flux, ω_s represents the synchronous speed, and indexes d and q stand for the direct and quadrature components.

2.4. The DFIG state-space model

From Eqs. (5) and (6), the current dynamics model of the DFIG under the stationary $(\alpha\beta)$ reference frame can be given by the following state-space form:

$$\frac{d\,x(t)}{dt} = A\,x(t) + B\,u(t), \tag{7}$$

by adopting the following notation:

$$x(t) = [i_{\alpha s}(t)\ i_{\beta s}(t)\ i_{\alpha r}(t)\ i_{\beta r}(t)]^T, \tag{8}$$

$$u(t) = [u_{\alpha s}(t)\ u_{\beta s}(t)\ u_{\alpha r}(t)\ u_{\beta r}(t)]^T, \tag{9}$$

where $x(t)$ is the state vector and $u(t)$ is a control vector. Thus, the state matrix A and the input matrix B can be given as follows:

$$A = A_0 + A_r \omega_r + A_s \omega_s, \tag{10}$$

where the matrices A_0, A_r, A_s, and B are respectively expressed as:

$$A_0 = \begin{bmatrix} -\frac{R_s}{\sigma L_s} & 0 & \frac{R_r L_m}{\sigma L_s L_r} & 0 \\[2mm] 0 & -\frac{R_s}{\sigma L_s} & 0 & \frac{R_r L_m}{\sigma L_s L_r} \\[2mm] \frac{L_m R_s}{\sigma L_s L_r} & 0 & -\frac{R_r}{\sigma L_r} & 0 \\[2mm] 0 & \frac{L_m R_s}{\sigma L_s L_r} & 0 & -\frac{R_r}{\sigma L_r} \end{bmatrix} \quad A_r = \begin{bmatrix} 0 & \frac{L_m^2}{\sigma L_s L_r} & 0 & \frac{L_m}{\sigma L_s} \\[2mm] -\frac{L_m^2}{\sigma L_s L_r} & 0 & -\frac{L_m}{\sigma L_s} & 0 \\[2mm] 0 & -\frac{L_m}{\sigma L_r} & 0 & -\frac{1}{\sigma} \\[2mm] \frac{L_m}{\sigma L_r} & 0 & \frac{1}{\sigma} & 0 \end{bmatrix}$$

$$A_s = \begin{bmatrix} 0 & 1 & 0 & 0 \\ -1 & 0 & 0 & 0 \\ 0 & 0 & 0 & 1 \\ 0 & 0 & -1 & 0 \end{bmatrix} \quad B = \begin{bmatrix} \frac{1}{\sigma L_s} & 0 & -\frac{L_m}{\sigma L_s L_r} & 0 \\ 0 & \frac{1}{\sigma L_s} & 0 & -\frac{L_m}{\sigma L_s L_r} \\ -\frac{L_m}{\sigma L_s L_r} & 0 & \frac{1}{\sigma L_r} & 0 \\ 0 & -\frac{L_m}{\sigma L_s L_r} & 0 & \frac{1}{\sigma L_r} \end{bmatrix}$$

with $\sigma = 1 - L_m^2/(L_s L_r)$.

3. Problem formulation

This section is devoted to investigating the proposed AFTTC scheme for the DFIG subject to actuator faults and noise measurement. Hence, the procedure of designing an AFTTC scheme is given in the following subsections.

3.1. Reference model of the DFIG

Consider a reference model of a DFIG in nominal function, which is defined as follows:

$$\begin{cases} \frac{dx(t)}{dt} = Ax(t) + Bu(t) \\ y(t) = Cx(t) \end{cases}, \tag{11}$$

where $x(t) \in \Re^n$ is the state vector, $y(t) \in \Re^p$ is the measured output vector, and $u(t) \in \Re^m$ is the control input vector. A, B, and C are constant real matrices defined by the state-space model.

3.2. Faulty model

We consider that the system of Eq. (11) is affected by actuator faults and noise measurement. The reference system of Eq. (11) can then be further rewritten in the following form:

$$\begin{cases} \frac{dx_f(t)}{dt} = A x_f(t) + B u_f(t) + E f_a(t) \\ y_f(t) = C x_f(t) + R d(t) \end{cases}, \tag{12}$$

where $x_f(t) \in \Re^n$, $y_f(t) \in \Re^p$, and $u_f(t) \in \Re^m$ are respectively the faulty state vector, the faulty output vector, and the fault tolerant control signal; $f_a(t) \in \Re^m$ represents the fault vector affecting the actuators, and $d(t) \in \Re^q$ denotes the noise measurement affecting the outputs. $E \in \Re^{n \times m}$ and $R \in \Re^{p \times q}$ are respectively the fault and noise distribution matrices, which are assumed to be known.

3.3. Assumptions

In order to guarantee the achievement of fault-tolerant aims, the following assumptions are employed throughout:

A1) The matrix A is a Hurwitz matrix.

A2) The system (A,C) is detectable $(rank\,[A,\ C]^T = n)$.

A3) The actuator faults $f_a(t)$ are assumed to be a bounded time-varying signal that is slowly time-varying.

3.4. The design of the PIO

The following structure of the PIO has the capability of providing simultaneous estimation of system states and actuator faults, which will be used for the design of the proposed AFTTC scheme. The latter can be given by [6,13]:

$$
\begin{cases}
\frac{d\hat{x}_f(t)}{dt} = A\,\hat{x}_f(t) + B\,u_f(t) + E\,\hat{f}_a(t) + K_p(y_f(t) - \hat{y}_f(t)) \\
\\
\frac{d\hat{f}_a(t)}{dt} = L_i(y_f(t) - \hat{y}_f(t)) \\
\hat{y}_f(t) = C\,\hat{x}_f(t)
\end{cases}
, \tag{13}
$$

where $\hat{x}_f(t) \in \Re^n$ is the estimated state, $\hat{f}_a(t) \in \Re^r$ represents the estimated actuator faults, $\hat{y}_f(t) \in \Re^m$ is the estimated output, and $K_p \in \Re^{n \times p}$ and $L_i \in \Re^{r \times p}$ are respectively the proportional gain and derivative gain matrices to be computed.

3.5. The proposed structure of the fault-tolerant controller law

The objective in this subsection is to design an AFTTC scheme that ensures the tracking of the faulty system state $x_f(t)$ in Eq. (12) to the nominal system state $x(t)$ in Eq. (11). The developed AFTTC scheme is based on the use of a PIO, as illustrated in Figure 3.
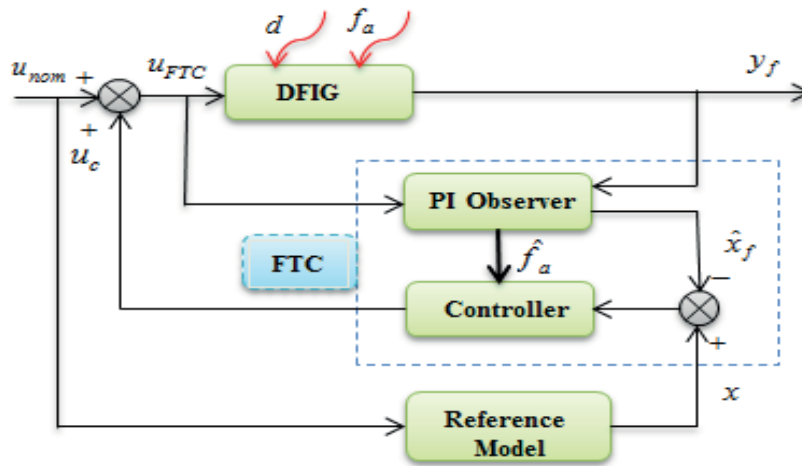

Figure 3. The architecture of the fault-tolerant control scheme.

The proposed structure of the fault-tolerant control law for the system of Eq. (11) is described by the following equations:

$$
\begin{cases}
u_{FTC}(t) = u_{nom}(t) + u_c(t) \\
u_c(t) = H_\mu(x(t) - \hat{x}_f(t)) - \hat{f}_a(t)
\end{cases}
, \tag{14}
$$

where u_{nom} is the nominal control input of the system without faults and u_c is a new added control vector, which is used to compensate the effect of actuator faults and to ensure the best tracking trajectory performance of the faulty system to the nominal system, and $H_\mu \in \Re^{r \times n}$ is a constant gain matrix to be computed for the design of the FTC.

3.6. The main LMI conditions for stability

In this section, the main objective is to propose novel sufficient LMI conditions that allow obtaining the gain matrices of the FTC (H_μ) and the PIO (L_i and K_p) values such that the previous assumptions are satisfied.

First, let us define the state tracking error, the state estimation, and the actuator fault estimation errors respectively as:

$$\begin{cases} e_t(t) = x(t) - x_f(t) \\ e_e(t) = x_f(t) - \hat{x}_f(t) \\ e_f(t) = f_a(t) - \hat{f}_a(t) \end{cases} . \tag{15}$$

By using Eqs. (11), (12), (13), and (14), and with some operations, the dynamics of $e_t(t)$, $e_t(t)$, and $e_f(t)$ are given respectively by the following equations:

$$\frac{d\,e_t(t)}{dt} = (A - B\,H_\mu)\,e_t(t) - B\,H_\mu\,e_e(t) - E\,e_f(t), \tag{16}$$

$$\frac{d\,e_e(t)}{dt} = (A - K_pC)e_e(t) + E\,e_f(t) - K_pR\,d(t), \tag{17}$$

$$\frac{d\,e_f(t)}{dt} = -L_iC\,e_f(t) + \frac{d\,f_a(t)}{dt} - L_iR\,d(t). \tag{18}$$

Eqs. (16), (17), and (18) are then combined in order to obtain the following augmented system:

$$\frac{d\,e_a(t)}{dt} = A_a\,e_a(t) + B_a\,\psi(t), \tag{19}$$

where $e_a(t)$ are the augmented variables, which can be expressed as:

$$e_a^T(t) = \begin{bmatrix} e_t^T(t) & e_e^T(t) & e_f^T(t) \end{bmatrix}, \tag{20}$$

and

$$A_a = \begin{bmatrix} (A - BH_\mu) & -B\,H_\mu & -E \\ 0 & (A - K_pC) & E \\ 0 & -L_iC & 0 \end{bmatrix}, \; B_a = \begin{bmatrix} 0 & 0 \\ -K_pR & 0 \\ -L_iR & I \end{bmatrix}, \; \Psi(t) = \begin{bmatrix} d(t) \\ \frac{df_a(t)}{dt} \end{bmatrix}.$$

The gain matrix H_μ, L_i, and K_p values are computed in order to ensure an asymptotic convergence of $e_a(t)$ towards zero when $\psi = 0$ and to guarantee a bounded error when $\psi \neq 0$ by solving the main LMI conditions, which are summarized in the following theorem.

Theorem. *The augmented system in Eq. (19) that generates the state tracking error $e_t(t)$, the state estimation $e_e(t)$, and the actuator faults $e_f(t)$ is stable and L_2-gain of the transfer from ψ to $e_a(t)$ is bounded, if there exist two symmetric and positive definite matrices $P_1 = P_1^T \in \Re^{n \times n}$, $P_2 = P_2^T \in \Re^{(n+r) \times (n+r)}$, with the matrices $X_1 \in \Re^{(m \times n)}$ and $X_2 \in \Re^{n \times (n+r)}$, such that the following LMI conditions hold:*

$$M_aA^T + A\,M_a - (B\,X_1)^T - (B\,X_1) < 0, \tag{21}$$

$$A_a^T\,P_2 + P_2\,A_a - (X_2\,C_a)^T - (X_2\,C_a) < 0. \tag{22}$$

The gain matrices of the FTC and the PIO are computed as follows:

$$\begin{cases} H_\mu = M_a^{-1} X_1 = P_1 X_1 \\ K = P_2^{-1} X_2 \end{cases}. \tag{23}$$

Proof See the theorem proof in the Appendix. □

4. Simulations and discussions

In this section, simulation results are presented to illustrate the efficiency of the proposed AFTTC scheme when different actuator faults occur. For such a purpose, two kinds of actuator fault scenarios are considered, a constant one and a time-varying one, and are carried out within the MATLAB/Simulink environment; parameters of the simulated DFIG and WT are given in [23].

Case 1: Simulation under constant actuator faults

In order to illustrate the efficiency of the proposed AFTTC scheme under constant actuator faults, we consider that all of the actuators are faulty, and each fault is defined respectively, as follows:

$$f_{a1} = \begin{cases} 1, & 0.3 \le t \le 0.5 \\ 0, & \text{else} \end{cases} \qquad f_{a2} = \begin{cases} 1, & 0.4 \le t \le 0.7 \\ 0, & \text{else} \end{cases}$$

$$f_{a3} = \begin{cases} 0.52, & 0.5 \le t \le 0.7 \\ 0, & \text{else} \end{cases} \qquad f_{a4} = \begin{cases} 0.42, & t \ge 0.55 \\ 0, & \text{else} \end{cases}$$

where f_{a1} occurs in $u_{\alpha s}$, f_{a2} occurs in $u_{\beta s}$, f_{a3} occurs in $u_{\alpha r}$, and f_{a4} occurs in $u_{\beta r}$.

The evolution of the state variables of the nominal system, the faulty system without AFTTC, and the faulty system with AFTTC are depicted in Figure 4, while Figure 5 shows the simulation results of the original constant faults with their estimation.

It is clear from Figure 4 that the proposed FTC is able to force the state of the system to track a reference state generated by a reference fault-free model, even in the presence of constant actuator faults. It is seen from Figure 5 that the estimated constant faults converge close to the original faults, which confirms that the designed PIO can provide an acceptable estimate of constant actuator faults.

Case 2: Simulation under time-varying actuator faults

In order to demonstrate the efficiency of the proposed AFTTC scheme when time-varying actuator faults occur, we consider that all of the actuators are affected by different time-varying faults, and each fault is defined respectively, as follows:

$$f_{a1} = \begin{cases} \sin(10\pi t) & 0.5 \le t \le 0.7 \\ 0 \end{cases} \qquad f_{a2} = \begin{cases} \sin(10\pi t) & 0.2 \le t \le 0.5 \\ 0 \end{cases}$$

$$f_{a3} = \begin{cases} 0.45\sin(10\pi t) & t \le 0.6 \\ ,0 \end{cases} \qquad f_{a4} = \begin{cases} 0.30\sin(5\pi t) & t \ge 0.5 \\ 0 \end{cases}$$

where f_{a1} occurs in $u_{\alpha s}$, f_{a2} occurs in $u_{\beta s}$, f_{a3} occurs in $u_{\alpha r}$, and f_{a4} occurs in $u_{\beta r}$.

From the simulation results, one can observe that the designed PIO and AFTTC schemes illustrate their efficiency, since the state trajectory tracking between the faulty system and the reference model is achieved,
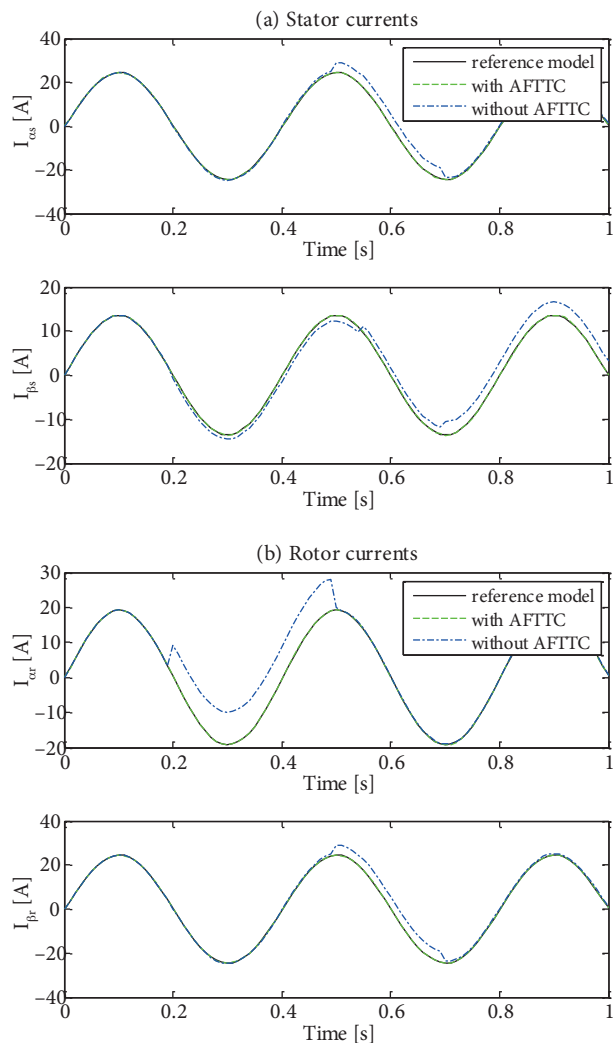
Figure 4. Comparison between the states: of the reference model, of the faulty system without AFTTC, and of the faulty system with AFTTC strategy.
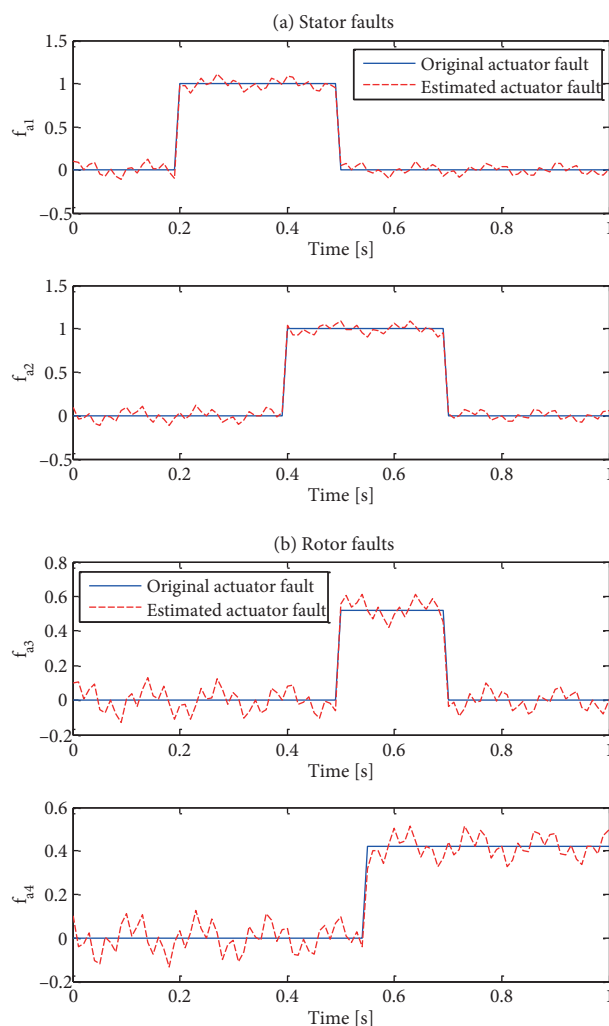
Figure 5. Constant actuator faults (f_{a1}, f_{a2}, f_{a3}, and f_{a4}) and their estimations.

even in the case of time-varying actuator faults (Figure 6). The estimated faults are closed to the original faults, as shown in Figure 7, which demonstrates that the PIO can provide an accurate estimation for time-varying faults. Finally, through these simulation tests, the results illustrate the efficiency and the effectiveness of the designed AFTTC scheme. It has a significant capacity of fault-tolerance control even when different kinds of actuator faults occur, which can allow the system to tolerate and compensate the fault effects to allow normal functioning of the system.

5. Conclusions and perspectives

This paper develops a novel strategy for an AFTTC scheme for a DFIG with actuator faults and noise measurement is proposed. This scheme is based on fault estimation and compensation using a PIO. The aim of the proposed strategy is to ensure the trajectory tracking for the state of the faulty system to a reference state generated by a reference fault-free model, to guarantee the stability of the whole closed-loop system when different faults occur. The main results are derived in terms of the LMIs, which can be readily solved with
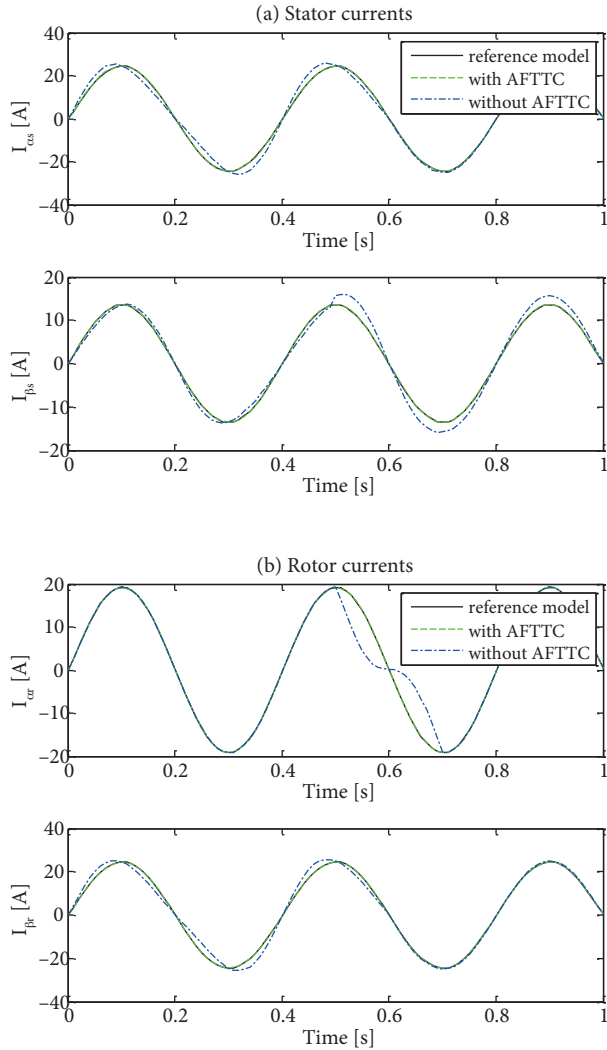
Figure 6. Comparison between the states: of the reference model, of the faulty system without AFTTC, and of the faulty system with AFTTC strategy.
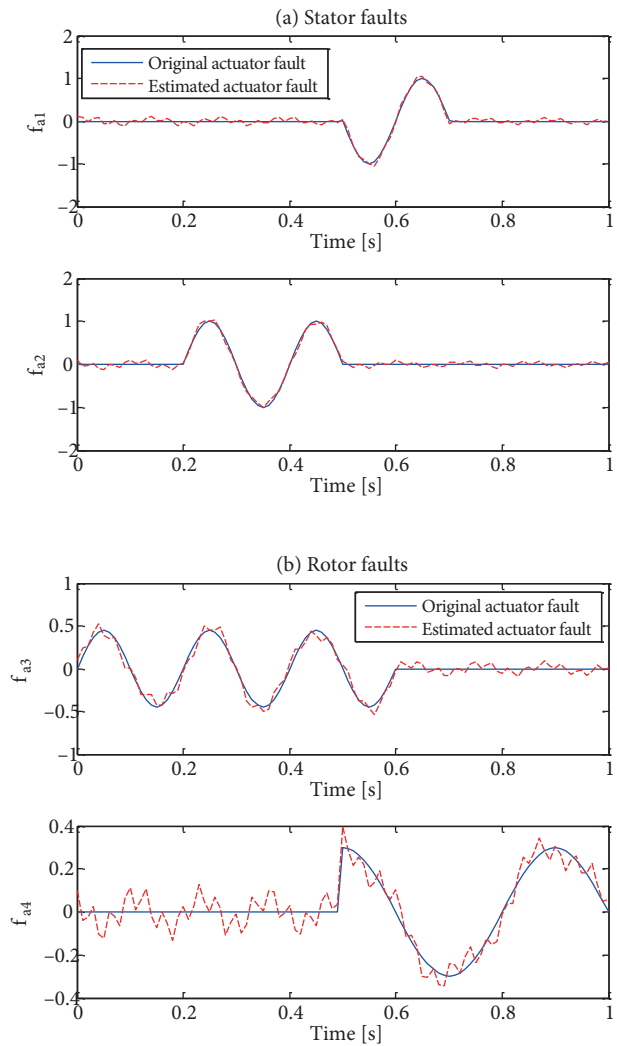
Figure 7. Time-varying actuator faults (f_{a1}, f_{a2}, f_{a3}, and f_{a4}) and their estimations.

the YALMIP toolbox and SeDuMi solver. Two kinds of actuator fault scenarios have been considered; the first scenario deals with constant actuator faults, and the second deals with time-varying actuator faults. The simulation results confirm that the proposed FTC scheme has a satisfactory effect to deal with constant and time-varying actuator faults. Future extensions of such a work include:

- Validating experimentally the proposed AFTTC scheme;

- Extending the results developed in this paper to the robust observer-based control design for uncertain systems with sensor faults and actuator faults;

- Applying the developed results for all WECSs.

References

[1] Perdana A, Carlson O, Persson J. Dynamic response of grid-connected wind turbine with doubly fed induction generator during disturbances. In: Nordic Workshop on Power and Industrial Electronics; 2004; Trondheim, Norway.

[2] Farhoodne M, Azah M, Shareef H, Zayandehroodi H. Power quality impacts of high-penetration electric vehicle stations and renewable energy-based generators on power distribution systems. Measurement 2013; 46: 2423-2434.

[3] Abdeddaim S, Betka A, Drid S, Becherif M. Implementation of MRAC controller of a DFIG based variable speed grid connected wind turbine. Energ Convers Manage 2014; 79: 281-288.

[4] Amundarain M, Alberdi M, Garrido A, Garrido I, de la Sen M. Neural control for wave power plant during voltage dips. Electr Pow Syst Res 2012; 92: 96-105.

[5] Chen S, Živanović R. Estimation of frequency components in stator current for the detection of broken rotor bars in induction machines. Measurement 2010; 43: 887-900.

[6] Abdelmalek S, Barazane L, Larabi A, Belmili H. Contributions to diagnosis and fault- tolerant control based on proportional integral observer: application to a doubly-fed induction generator. In: IEEE 2015 4th International Conference on Electrical Engineering; 13–15 December 2015; Boumerdes. Algeria. New York, NY, USA: IEEE. pp. 1-5.

[7] Benbouzid M, Beltran B, Amirat Y, Yaoc G, Han J, Mangel H. Second-order sliding mode control for DFIG-based wind turbines fault ride-through capability enhancement. ISA Trans 2014; 53: 827-833.

[8] Elkhatib K, Aitouche A, Abbes D. Robust fuzzy scheduler fault tolerant control of wind energy systems subject to sensor and actuator faults. Electr Pow Energ Syst 2014; 55: 402-419.

[9] Wu LB, Yang GH, Ye D. Robust adaptive fault-tolerant control for linear systems with actuator failures and mismatched parameter uncertainties. IET Contr Theor Appl 2014; 8: 441-449.

[10] Zhang K, Jiang B, Shi P. Fast fault estimation and accommodation for dynamical systems. IET Contr Theor Appl 2009; 3: 189-199.

[11] Zhang K, Jiang B, Staroswiecki M. Dynamic output feedback fault-tolerant controller design for Takagi–Sugeno fuzzy systems with actuators faults. IEEE T Fuzzy Syst 2010; 18: 194-201.

[12] Djeghali N, Ghanes M, Djennoune S, Barbot JP. Sensorless fault tolerant control for induction motors. Int J Control Autom Syst 2013; 11: 563-576.

[13] Aouaouda S, Chadli M, Tarek KM, Bouarar T. Robust fault tolerant tracking controller design for unknown inputs T–S models with unmeasurable premise variables. J Proc Contr 2012; 22: 861-872.

[14] Djamel B, Dalel J, Ilhem K. Fault-tolerant control for a class of switched linear systems using generalized switched observer scheme. J Contr Eng Appl Informatics 2015; 17: 90-101.

[15] Simani S, Castaldi P. Active actuator fault-tolerant control of a wind turbine benchmark model. Int J Rob Nonlin Contr 2014; 24: 1283-1303.

[16] Jiang J, Yu X. Fault-tolerant control systems: a comparative study between active and passive approaches. Annu Rev Contr 2012; 36: 60-72.

[17] Sloth C, Esbensen T, Stoustrup J. Robust and fault-tolerant linear parameter-varying control of wind turbines. Mechatronics 2011; 21: 645-659.

[18] Shi F, Patton R. An active fault-tolerant control approach to an offshore wind turbine model. Renew Energ 2015; 75: 788-798.

[19] Wang X, Wang Y, Zhicheng J, Dinghui W. Design of two-frequency-loop robust fault- tolerant controller for wind energy conversion systems. In: IEEE 2010 Industrial Electronics and Applications conference; 15–17 June 2010; Taichung, Taiwan. New York, NY, USA: IEEE. pp. 718-723.

[20] Wang Y, Zhou D, Qin SJ, Wang H. Active fault-tolerant control for a class of nonlinear systems with sensor faults. Int J Control Autom Syst 2008; 6: 339-350.

[21] Wei X, Verhaegen M, Van-den-Engelen T. Sensor fault detection and isolation for wind turbines based on subspace identification and Kalman filter techniques. Int J Adapt Contr Sign Proc 2010; 24: 687-707.

[22] Wei X, Verhaegen M, Van-den-Engelen T. Sensor fault diagnosis of wind turbines for fault- tolerant. In: Proceedings of the 17th world Congress of the International Federation of Automatic Control; July 2008; Seoul, South Korea. pp. 3222-3227.

[23] Elkhatib K, Aitouche A, Ghorbani R, Bayart M. Robust fuzzy fault-tolerant control of wind energy conversion systems subject to sensor faults. IEEE T Sustain Energ 2012; 3: 231-241.

[24] Elkhatib K, Oueidat M, Aitouche A, Ghorbani R. Robust scheduler fuzzy controller of DFIG wind energy systems. IEEE T Sustain Energ 2013; 4: 706-715.

[25] Montadher S, Patton RJ. Fault-tolerant adaptive sliding mode controller for wind turbine power maximisation. In: Proceedings of the 7th IFAC Symposium on Robust Control Design; 20–22 June 2012; Aalborg Congress & Culture Centre, Denmark. pp. 499-504.

[26] Montadher S, Patton RJ. Wind turbine power maximization based on adaptive sensor fault-tolerant sliding mode control. In: IEEE 2012 Control & Automation Conference; 3–6 July 2012; Barcelona, Spain. New York, NY, USA: IEEE. pp. 1183-1188.

[27] Li H, Yang C, Hu YG, Zhao B, Zhao M, Chen Z. Fault-tolerant control for current sensors of doubly fed induction generators based on an improved fault detection method. Measurement 2014; 47: 929-937.

[28] Montadher SS, Patton RJ. Active sensor fault- tolerant output feedback tracking control for wind turbine systems via T–S model. Eng Appl Artif Intel 2014; 34: 1-12.

[29] Mengi OÖ, Altaş İH. Fuzzy logic control for a wind/battery renewable energy production system. Turk J Elec Eng & Comp Sci 2012; 20: 187-206.

[30] Karakaya A, Karakaş E. Implementation of neural network-based maximum power tracking control for wind turbine generators. Turk J Elec Eng & Comp Sci 2014; 22: 1410-1422.

[31] Şahin ME, Sharaf AM, Okumuş Hİ. A novel filter compensation scheme for single phase self-excited induction generator micro wind generation system. Scientific Research and Essays 2012; 7: 3058-3072.

Appendix. Proof of the theorem.

The aim here is to demonstrate the quadratic stability of the augmented system of Eq. (19), which means to ensure an asymptotic convergence of $e_a(t)$ towards zero when $\psi = 0$ and to guarantee a bounded error when $\psi \neq 0$. For this reason, we consider the following candidate Lyapunov candidate function $V(e_a(t))$ for the augmented system of Eq. (19). In this case, the problem is reduced to finding P verifying $V < 0$.

$$V(e_a(t)) = e_a(t)^T P\, e_a(t),\ P = P^T > 0 \tag{A.1}$$

Here P is structured as follows:

$$P = \begin{bmatrix} P_1 & 0 \\ 0 & P_2 \end{bmatrix},\quad P_1 > 0 \text{ and } P_2 > 0 \tag{A.2}$$

By differentiating Eq. (A.1), we obtain:

$$\frac{d\,V(e_a(t))}{dt} = \frac{d\,e_a^T(t)}{dt} P\, e_a(t) + e_a^T(t) P\, \frac{d\,e_a^T(t)}{dt} < 0 \tag{A.3}$$

From Eqs. (A.1) and (A.2), Eq. (A.3) becomes:

$$\frac{d\,V(e_a(t))}{dt} = e_a^T(t)(\,A_0^T\,P +\ PA_0)e_a(t) < 0 \tag{A.4}$$

The error $e_a(t)$ converges to zero if Eq. (A.4) is verified if:

$$A_0^T\,P +\ PA_0 < 0 \tag{A.5}$$

Here the matrices A_0 and B_0 can be given as:

$$A_0 = \begin{bmatrix} A - B\,H_\mu & E_1 \\ 0 & A_{a1} - K\,C_{a1} \end{bmatrix}, B_0 = \begin{bmatrix} 0 \\ I_a - K\,D_a \end{bmatrix}$$

and

$$A_{a1} = \begin{bmatrix} A & E \\ 0 & 0 \end{bmatrix},\quad K = \begin{bmatrix} K_p \\ L_I \end{bmatrix},\quad I_a = \begin{bmatrix} 0 & 0 \\ 0 & I \end{bmatrix}, C_{a1} = \begin{bmatrix} C \\ 0 \end{bmatrix}^T,\quad D_a = \begin{bmatrix} D \\ 0 \end{bmatrix}^T,\quad E_a = \begin{bmatrix} -B\,H_\mu \\ -E \end{bmatrix}^T$$

Therefore, Eq. (A.5) is equivalent to the following inequalities:

$$(A - B\,H_\mu)^T P_1 +\ P_1\ (A - B\,H_\mu) < 0 \tag{A.6}$$

$$(A_{a1} - K\,C_{a1})^T\,P_2 +\ P_2\ (A_{a1} - K\,C_{a1}) < 0 \tag{A.7}$$

Then, left and right multiplying the latter condition (Eq. (A.6)) by P_1^{-1}, and considering the following change of variable $M_a = P_1^{-1}$, we can get:

$$M_aA^T +\ A\,M_a - (B\,H_\mu)^T P_1 - P_1(B\,H_\mu) < 0 \tag{A.8}$$

$$A_{a1}^T P_2 + P_2\, A_{a1} - (K\, C_{a1})^T P_2 - P_2(K\, C_{a1}) < 0 \tag{A.9}$$

Eqs. (A.8) and (A.9) are a set of nonlinear matrix inequalities and for the convenience of design should be transformed into pure LMIs by applying the change of variables $X_1 = M_a H_\mu$ and $X_2 = P_2 K$. One can thus obtain the following LMIs:

$$M_a A^T + A\, M_a - (B\, X_1)^T - (B\, X_1) < 0 \tag{A.10}$$

$$A_{a1}^T P_2 + P_2\, A_{a1} - (X_2\, C_{a1})^T - (X_2\, C_{a1}) < 0 \tag{A.11}$$

Solving the LMIs of Eqs. (A.10) and (A.11) allows us to find the gain matrices M_a, P_2, X_1, and X_2. The gain matrices of the fault tolerant controller (H_μ) and the proportional integral observer (K) are then computed by:

$$\begin{cases} H_\mu = M_a^{-1} X_1 = P_1 X_1 \\ K = P_2^{-1} X_2 \end{cases} \tag{A.12}$$